

AD-A123 569

SATURATION OF THE LOWER-HYBRID-DRIFT INSTABILITY BY  
MODE COUPLING(U) NAVAL RESEARCH LAB WASHINGTON DC  
J P DRAKE ET AL. 26 JAN 83 NRL-MR-5009

1/1

UNCLASSIFIED

F/G 20/9

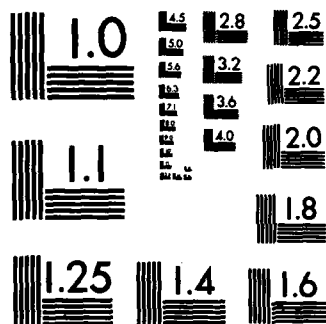
NL

END

41.0000

204

DTIC



MICROCOPY RESOLUTION TEST CHART  
NATIONAL BUREAU OF STANDARDS-1963-A

ADA 123569

SECURITY CLASSIFICATION OF THIS PAGE (When Data Entered)

REPORT DOCUMENTATION PAGE		READ INSTRUCTIONS BEFORE COMPLETING FORM
1. REPORT NUMBER NRL Memorandum Report 5009	2. GOVT ACCESSION NO. <b>A123 569</b>	3. RECIPIENT'S CATALOG NUMBER
4. TITLE (and Subtitle) SATURATION OF THE LOWER-HYBRID-DRIFT INSTABILITY BY MODE COUPLING	5. TYPE OF REPORT & PERIOD COVERED Interim report on a continuing NRL problem.	
7. AUTHOR(s) J.F. Drake*, P.N. Guzdar,† and J.D. Huba	6. PERFORMING ORG. REPORT NUMBER	
9. PERFORMING ORGANIZATION NAME AND ADDRESS Naval Research Laboratory Washington, DC 20375	10. PROGRAM ELEMENT, PROJECT, TASK AREA & WORK UNIT NUMBERS 61153N; RR033-02-44; 47-0884-0-3; 47-1447-0-3	
11. CONTROLLING OFFICE NAME AND ADDRESS Office of Naval Research      NASA Arlington, VA 22217      Washington, DC	12. REPORT DATE January 26, 1983	
14. MONITORING AGENCY NAME & ADDRESS (if different from Controlling Office)	13. NUMBER OF PAGES 10	
	15. SECURITY CLASS. (of this report) UNCLASSIFIED	
	16. DECLASSIFICATION/DOWNGRADING SCHEDULE	
18. DISTRIBUTION STATEMENT (of this Report)  Approved for public release; distribution unlimited.		
17. DISTRIBUTION STATEMENT (of the abstract entered in Block 20, if different from Report)  DTIC COPY INSPECTED 2 <b>A</b>		
19. SUPPLEMENTARY NOTES *Present address: University of Maryland, College Park, MD 20742 †Present address: Science Applications, Inc., McLean, VA 22102 This research was supported by the Office of Naval Research, NASA, and partially by the Department of Energy.		
19. KEY WORDS (Continue on reverse side if necessary and identify by block number)  Lower-hybrid-drift instability      Plasma stability Nonlinear plasma theory      Mode coupling		
20. ABSTRACT (Continue on reverse side if necessary and identify by block number)  A nonlinear mode-coupling theory of the lower-hybrid-drift instability is presented. A 2-D mode equation is derived which includes the nonlinear polarization and $E \times B$ electron drifts, adiabatic ions, and realistic sources and sinks of energy. It is found that the instability saturates by transferring energy from the growing, long wavelength modes to the damped, short wavelength modes. The saturation energy, mean square of the potential fluctuations, and diffusion coefficient are calculated self-consistently.		

DD FORM 1473

EDITION OF 1 NOV 65 IS OBSOLETE  
S/N 0102-014-6601

SECURITY CLASSIFICATION OF THIS PAGE (When Data Entered)

## SATURATION OF THE LOWER-HYBRID-DRIFT INSTABILITY BY MODE COUPLING

A first principles theory of the nonlinear saturation of the lower-hybrid-drift instability and associated particle transport is presented. A nonlinear equation describing 2-D lower-hybrid-drift turbulence is derived which includes the nonlinear  $\vec{E} \times \vec{B}$  and polarization drifts of the electrons, adiabatic ions, and realistic sources and sinks of energy. The equation is solved numerically to obtain the evolution and saturation of the wave spectrum, as well as the self-consistent particle flux which yields the diffusion coefficient.

The lower-hybrid-drift instability is a flute mode ( $\vec{k} \cdot \vec{B} = 0$ ) which is driven unstable in a plasma with strong inhomogeneities,  $\rho_i/L_n > (m_e/m_i)^{1/4}$ , where  $\rho_i$  and  $L_n$  are the ion Larmor radius and density scale length, respectively. The linear behavior of the instability is well understood.<sup>1,2</sup> In the weak drift regime ( $V_{di} < v_i$ , where  $V_{di} = v_i^2/2\Omega_i L_n$  is the ion diamagnetic drift velocity and  $v_i$  is the ion thermal velocity) the mode is driven unstable by the resonant interaction of the wave with the drifting ions when  $\omega/k_y < V_{di}$ . The growth rate maximizes at  $k_y \sim \rho_{es}^{-1} \equiv \rho_i^{-1}(m_i/m_e)^{1/2}$ . The mode is stable for  $k_y \rho_{es} \gg 1$ , and approaches marginal stability as  $k_y \rho_{es} \rightarrow 0$ .<sup>3</sup> The wave frequency is such that  $\Omega_i \ll \omega \ll \Omega_e$  so that the electrons are strongly magnetized while the ions can be treated as unmagnetized. In a finite  $\beta$  plasma the resonant interaction of VB drifting electrons with the wave is stabilizing.

The nonlinear behavior of the instability is much less well understood. Ion trapping has been observed to quench the growth of the instability in particle simulations.<sup>4</sup> The onset of stochastic electron heating has also been proposed to explain saturation in these simulations.<sup>5</sup> On the other hand, ion trapping is not a viable saturation mechanism when a broad 2-D spectrum of waves is excited, and it has not been observed in recent simulations using realistic mass ratios where such spectra develop.<sup>6</sup> In this letter we focus on the nonlinear coupling of stable and unstable waves to saturate the instability.

We consider a slab equilibrium of cold electrons and warm ions with a density profile  $n_0(x)$  supported by a magnetic field  $B_{z0}(x)$ . The equilibrium ion velocity distribution is taken to be a Maxwellian with an average drift velocity  $\vec{V}_i = V_{di} \hat{e}_y$ . Because of the flute nature of the instability ( $\vec{k} \cdot \vec{B} = 0$ ), we self-consistently limit the spatial variations

to the xy plane (as contrasted with universal drift-wave turbulence which is inherently 3-D). In the weak drift regime the ions respond to the perturbed potential  $\phi(x,y,t)$  adiabatically to lowest order since  $\omega \ll kv_1$ . Thus,

$$n_1 = n_0 \left[ 1 + \sqrt{\pi} v_1^{-1} |\nabla^{-1}| \left( \frac{\partial}{\partial t} + v_{di} \frac{\partial}{\partial y} \right) \right] \exp(-e\phi/T_1) \quad (1)$$

where the term proportional to  $\sqrt{\pi}$  in (1) is a small correction describing the resonant ion interaction. The perturbed electron motion is simply given by the  $\underline{E} \times \underline{B}$  and polarization drifts,

$$\underline{v}_e = \frac{c}{B} \nabla \phi \times \hat{e}_z - \frac{c}{B\Omega_e} \frac{d}{dt} \nabla \phi \quad (2)$$

where  $d/dt = \partial/\partial t + \underline{v}_e \cdot \nabla$ . Using (2), the electron continuity equation can be written as

$$\frac{d}{dt} \ln n_e = -\rho_{es}^2 \frac{d}{dt} \nabla^2 (e\phi/T_1) \quad (3)$$

Finally, invoking charge neutrality ( $n_e = n_1$ ) and combining (1) and (3), we obtain the nonlinear equation

$$\begin{aligned} (1 - \hat{\nabla}^2) \hat{\phi}_\tau + \hat{\phi}_y - \gamma_0 |\nabla^{-1}| (\hat{\phi}_{\tau\tau} + \hat{\phi}_{\tau y}) + \gamma_e \hat{\phi} \\ + (\nabla \hat{\phi} \times \hat{e}_z \cdot \nabla) \nabla^2 \hat{\phi} + \gamma_0 \nabla \hat{\phi} \times \hat{e}_z \cdot \nabla |\nabla^{-1}| (\hat{\phi}_\tau + \hat{\phi}_y) = 0 \end{aligned} \quad (4)$$

where  $\hat{\nabla} = \rho_{es} \nabla$ ,  $\tau = (\rho_{es}/L_n) \Omega_e t$ ,  $\hat{\phi} = (e\phi/T_1)(L_n/\rho_{es})$  and the subscripts on  $\hat{\phi}$  denote a derivative with respect to that variable. The quantity  $\gamma_e$  represents the wave damping due to VB resonant electrons in a finite  $\beta$  plasma. Equation (4) is only valid for  $\gamma_0 = \pi^{1/2} v_{di}/v_1 < 1$  since the adiabatic ion response can only be justified in this limit. Linearizing this equation, we obtain the complex eigenvalue (in our normalized units),

$$\hat{\omega} = \hat{\omega}_k = \frac{\hat{k}_y}{1+\hat{k}^2} + i\gamma_0 \frac{\hat{k}^2 |\hat{k}|}{(1+\hat{k}^2)^3} - i\gamma_e \frac{1}{1+\hat{k}^2} \quad (5)$$

In the limit  $\gamma_e, \gamma_0 \rightarrow 0$ , (4) reduces to the Hasegawa-Mima equation in which the nonlinearity arises from the nonlinear polarization drift.<sup>7</sup> This equation has two invariants, energy and enstrophy, neither of which is preserved in the more general (4). When  $\gamma_0$  is finite, the  $\mathbf{E} \times \mathbf{B}$  nonlinearity also appears in (4). This nonlinearity has been considered by Horton<sup>8</sup> and, more recently by Waltz,<sup>9</sup> in studying universal mode turbulence. However, our equation differs from their work in that we do not assume that  $\hat{\phi}_x + \hat{\phi}_y$  is replaced by its linear counterpart  $-i(\hat{\omega}_k - k_y)\hat{\phi}$ . Thus, our equation is second order in time rather than first order.

The direction of energy flow described by (4) can be understood by calculating the stability of a single large amplitude wave  $\phi_0$  with  $\hat{k}_0$  and  $\hat{\omega}_0$  satisfying (5). A perturbation of wavevector  $\hat{k}$  is coupled through the pump to modes with  $\hat{k} \pm p\hat{k}_0$  ( $p = 1, 2, \dots$ ). For simplicity, we consider only the coupling of  $(\hat{\omega}, \hat{k})$  with its nearest neighbors  $(\hat{\omega}_\pm, \hat{k}_\pm)$  where  $\hat{\omega}_\pm = \hat{\omega} \pm \hat{\omega}_0$  and  $\hat{k}_\pm = \hat{k} \pm \hat{k}_0$ , i.e.,  $p=1$ . The dispersion relation for this  $(\hat{k}, \hat{k}_\pm)$  coupled system is

$$\varepsilon(\hat{k}, \hat{\omega}) + |\phi_0|^2 \left[ \frac{M(\hat{k}_0, \hat{k}_\pm)M(\hat{k}, \hat{k}_0)}{\varepsilon(\hat{k}_\pm, \hat{\omega}_\pm)} + (\hat{k}_0 + \hat{k}_\pm) \right] = 0 \quad (6)$$

where  $\varepsilon(\hat{k}, \hat{\omega}) = \hat{\omega}[1 + \hat{k}^2(1 - i\delta_k)] - k_y + i\gamma_e$ ,  $\delta_k = \gamma_0(k_y - \hat{\omega})/\hat{k}^3$  and  $M(\hat{k}_1, \hat{k}_2) = \hat{k}_1 \times \hat{k}_2 \cdot \hat{e}_z [k_1^2(1 - i\delta_{k1}) - k_2^2(1 - i\delta_{k2})]$ . When  $\gamma_0$  and  $\gamma_e$  are neglected in (6) and we take the limit  $\hat{\omega} \gg \hat{\omega}_k$ , the decay modes are purely growing with a growth rate which peaks around  $\hat{k} \cdot \hat{k}_0 \approx 0$  with  $|\hat{k}| < |\hat{k}_0|$ . A necessary requirement for instability is that one of the decay waves  $(\hat{k}, \hat{k}_\pm)$  has a longer wavelength than the pump. For this situation, in which (4) reduces to the Hasegawa-Mima equation, the wave energy inevitably cascades to longer and longer wavelength so that no stationary wave spectrum can result.<sup>10</sup> When  $\gamma_0$  is included, this conclusion no longer remains valid. Taking the limit  $|\hat{k}_0| \ll |\hat{k}|$  and again assuming  $\hat{\omega} \gg \hat{\omega}_k$ , the dispersion relation is given by

$$\hat{\omega}^2 = \frac{2|\phi_0|^2 (\hat{k} \times \hat{k}_0 \cdot \hat{e}_z)^2 \hat{k}^4}{1 + \hat{k}^2} \left[ 1 + i \frac{\gamma_0 \hat{\omega} (2 + \hat{k}^2)}{|\hat{k}|^3 (1 + \hat{k}^2)} \right]. \quad (7)$$

Equation (7) yields a dissipative instability which is driven unstable by

the  $\underline{E} \times \underline{B}$  nonlinearity. This instability produces a flow of energy from long to short wavelengths and, as will be demonstrated, enables the wave spectrum to reach a steady state.

We solve (4) numerically by decomposing it into two coupled, first-order (in time) differential equations which are advanced in time. These equations are solved by a spectral method developed by Fyfe et al.,<sup>11</sup> based on the work of Orzag.<sup>12</sup> The potential  $\hat{\phi}$  is Fourier-decomposed, i.e.,  $\hat{\phi} \sim \exp(i\mathbf{k} \cdot \mathbf{x})$  where  $\mathbf{k} = \mathbf{n}/\lambda$  and  $\mathbf{n} = n_x \hat{\mathbf{e}}_x + n_y \hat{\mathbf{e}}_y$  with  $n_x$  and  $n_y$  integers, and  $\lambda = 5$  (which fixes the  $|\mathbf{n}|$  for which  $|\mathbf{k}| = 1$ ). The numerical results presented in this letter are nominally computed on a  $32 \times 32$  mesh.

The electron damping  $\gamma_e$  controls the region of instability in  $\mathbf{k}$  space by stabilizing short wavelength modes. We have chosen

$$\gamma_e = \gamma_0 |\hat{\mathbf{k}}|^7 (1 + \hat{k}^2)^{-2} k_m^{-4} \quad (8)$$

with  $k_m = 1.6$ , which yields an unstable wave spectrum which is realistic for the lower-hybrid-drift instability in finite  $\beta$  plasmas. The growth rate peaks at  $(\hat{k}_x, \hat{k}_y) = (0, \pm 1)$  and is stable for  $\hat{k}_y > 1.6$  and  $\hat{k}_x > 1$ .

The  $\hat{\phi}$  spectrum is initialized with random noise with  $\hat{\phi} \sim 10^{-2} - 10^{-3}$ , and the system is allowed to evolve until the wave energy, given by

$$W/nT = (m_e/\pi m_i) \gamma_0^2 \sum_{\mathbf{k}} (1 + \hat{k}^2) |\hat{\phi}_{\mathbf{k}}|^2 \quad (9)$$

reaches a steady state value. The mean square of the potential fluctuations,

$$P = \langle (e\phi/T)^2 \rangle^{1/2} = [(2m_e/\pi m_i) \gamma_0^2 \sum_{\mathbf{k}} |\hat{\phi}_{\mathbf{k}}|^2]^{1/2} \quad (10)$$

as well as the nonlinear and quasilinear diffusion coefficients

$$\hat{D}_{nl} = D_{nl}/v_{es} \rho_{es} = (2m_e/\pi m_i)^{1/2} \gamma_0^2 \sum_{\mathbf{k}} (\hat{k}_y/|\hat{\mathbf{k}}|) \hat{\phi}_{\mathbf{k}}^* (\hat{k}_y \hat{\phi}_{\mathbf{k}} - i \frac{\partial \hat{\phi}_{\mathbf{k}}}{\partial \tau}) \quad (11)$$

$$\hat{D}_{ql} = D_{ql}/v_{es} \rho_{es} = (2m_e/\pi m_i)^{1/2} \gamma_0^2 \sum_{\mathbf{k}} |\hat{\mathbf{k}}|^2 \hat{k}_y^2 |\hat{\phi}_{\mathbf{k}}|^2 (1 + \hat{k}^2)^{-1} \quad (12)$$

respectively, are also computed. The nonlinear diffusion coefficient  $\hat{D}_{nl}$



is derived by averaging the particle flux in the  $x$  direction over  $y$ , i.e.,  $\hat{D}_{nl} \propto \langle nV_x \rangle_y$ . The quasilinear expression is then obtained by approximating  $\partial/\partial\tau = -i\omega_k$  and using (5) in (11).

In Fig. 1 we show instantaneous 2-D wave spectra in  $n$  space for  $\gamma_0 = .5$ . Figure 1a shows the spectrum during the linear phase of the instability, and Fig. 1b shows the spectrum after saturation. In the linear regime, the wave spectrum is strongly peaked around the most unstable modes,  $(n_x, n_y) = (0, \pm 5)$ . The spectrum begins to saturate as these modes couple through a  $n_y = 0$  mode (typically with  $n_x \sim 4$ ) to damped modes with  $n_x \geq n_y$ . A peak in the wave spectrum appears around  $(4, 0)$  at this time. This transient phase is completed as the total wave energy saturates and spreads through most of the unstable, weakly damped volume of  $n$  space as shown in Fig. 1b. The spectrum typically remains peaked around  $n_x \sim 0$  with  $n_y$  typically somewhat smaller than that of the linearly most unstable mode [see Fig. 1b for which the dominant modes are  $(n_x, n_y) = (0, \pm 3)$ ]. The 2-D wave spectrum exhibits substantial variability in time, even after saturation, as the unstable and stable modes continue to exchange energy in a dynamic manner.

The time evolution of the total wave energy ( $W$ ), mean square of the potential fluctuations ( $P$ ), and the nonlinear ( $\hat{D}_{nl}$ ) and quasilinear diffusion ( $\hat{D}_{ql}$ ) coefficients are shown in Fig. 2. All of these quantities exhibit a similar temporal behavior. The initial decay ( $\tau < 4$ ) is associated with the rapid dissipation of energy initialized in the damped modes, and is followed by a linear growth phase ( $4 < \tau < 20$ ). Subsequently, mode coupling occurs which leads to saturation of the instability, albeit with some initial overshoot ( $\tau \sim 24$ ). The levels of the total wave energy and other parameters of Fig. 2 are quite stationary in time after saturation. Also, the stationary values of all four quantities are relatively insensitive to the initialization of  $\phi$ .

We note that in Fig. 2, the quasilinear diffusion coefficient ( $\hat{D}_{ql}$ ) tracks the actual, nonlinear diffusion coefficient ( $\hat{D}_{nl}$ ) quite well during the entire time evolution of the instability. An important point which must be emphasized with regard to  $\hat{D}_{nl}$  is that both species, electrons and ions, continue to exchange both energy and momentum even after a steady state is reached; the electrons through the VB resonance and the ions by

direct resonant interaction. If the instability had saturated by ion trapping and the electrons had no resonant interaction with the wave, there would be no diffusion in the steady state since the electrons could not exchange momentum with the ions. Both species must have a dissipative interaction with the waves to have diffusion.

A number of runs have been made for different values of  $\gamma_0$ , the drift parameter. The saturation level of  $\hat{\phi}$  is found to be nearly independent of  $\gamma_0$ . Thus, from Eqs. (11) and (12), it is found that  $\hat{D}_{n1} = \gamma_0^2 = v_{di}^2/v_i^2$ .

Next, we compare our stationary values of  $P$  and  $\hat{D}_{n1}$  with those obtained from "wave energy bound" calculations.<sup>13</sup> The "energy bound" results from equating the wave energy with the kinetic energy associated with the relative drift of the electrons and ions,  $m_e n (V_{di} - V_{de})^2/2$ . This free energy bound is actually an extreme underestimate of the free energy in a finite  $\beta$  plasma, since the instability can also feed off the magnetic free energy, which typically greatly exceeds the drift energy.<sup>14</sup> Nevertheless, this bound has been widely invoked and seems to yield reasonable transport rates when compared with experimental observations. The "drift energy bound" yields a potential  $P_{eb} = (m_e/\pi m_i)^{1/2} \gamma_0$ , where we have assumed  $T_e \ll T_i$ . The scaling of  $P_{eb}$  is identical with that given in (10) since  $\hat{\phi}$  is independent of  $\gamma_0$ . For the case  $\gamma_0 = .5$ ,  $P/P_{eb} = 3$  (from Fig. 2) so that the actual fluctuation level obtained from our code is slightly larger than calculated from the "energy bound". Finally we compare  $\hat{D}_{n1}$  with that obtained from the simple formula  $\hat{D} = (\gamma/k^2)/v_{es}^0$ , where  $\gamma$  and  $k$  are evaluated where  $\gamma$  peaks. We find  $\hat{D} = (m_e/\pi m_i)^{1/2} \gamma_0^2$ , which again has the same scaling as  $\hat{D}_{n1}$  but is a factor of 2.4 smaller for  $\gamma_0 = 0.5$  (from Fig. 2).

Measurements of lower-hybrid-drift turbulence in a  $\theta$ -pinch by  $CO_2$  laser scattering have been reported recently.<sup>15</sup> The observed wave spectra were flute-like ( $\mathbf{k} \cdot \mathbf{B} \approx 0$ ) with clear peaks around  $\hat{k}_y \approx 0.7$  (a factor of two smaller than the most unstable linear mode), and  $\hat{k}_x < \hat{k}_y$ . Data was taken for three different filling pressures, corresponding to three values of  $v_{di}/v_i$ . Electron-ion collisions were apparently significant [ $\nu_{ei} \sim (\Omega_e \Omega_i)^{1/2}$ ] for the two highest filling pressures so we can only compare our results with the data from the lowest filling pressure, which corresponds to  $v_{di}/v_i = 0.52$  ( $\gamma_0 \approx 0.9$ ). The measured density fluctuation,

$\tilde{n}/n_0 \sim 0.014$ , is quite close (smaller by a factor of 2) to our theoretical prediction of  $\tilde{n}/n_0 \approx 0.025$ . In addition, the shift to long wavelength is consistent with our calculated spectra (compare Figs. 1a and 1b).

Computer simulations of the lower-hybrid-drift instability with realistic mass ratios have also been performed recently using a fluid-kinetic numerical scheme.<sup>6</sup> Unfortunately, these computations have been carried out for  $V_{di}/v_i > 1$ , which is outside the range of validity of our present theory. Nevertheless, a broad spectrum of modes is observed in  $k$  space in the simulations which is consistent with our calculations.

In conclusion, the lower-hybrid-drift instability can saturate via a mode coupling process. The basic saturation mechanism involves a transfer of energy from the growing, long wavelength modes to the damped, short wavelength modes. The nonlinear  $\underline{E} \times \underline{B}$  drift plays a crucial role in this saturation mechanism by preventing the polarization drift nonlinearity from driving the wave energy towards the undamped, long wavelength modes. The saturation energy and diffusion coefficient associated with the wave turbulence scales as  $(V_{di}/v_i)^2$ .

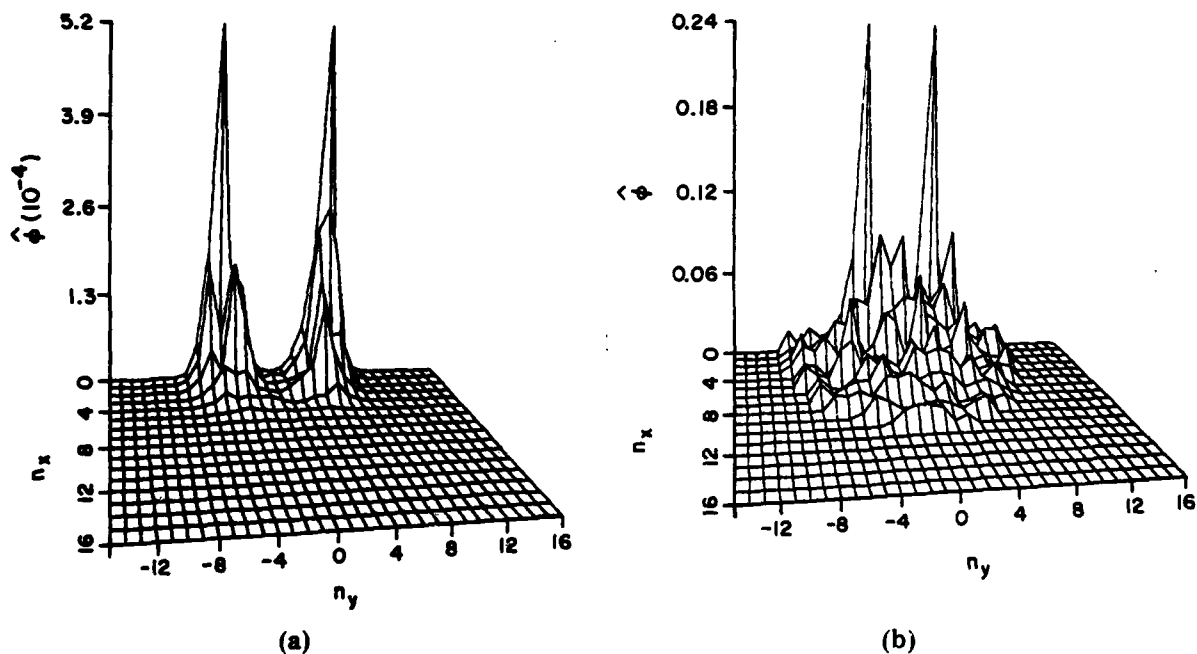


Fig. 1. Instantaneous 2D wave spectra of lower-hybrid-drift wave turbulence. (1a) Linear stage: The dominant linear modes are  $(n_x, n_y) = (0, \pm 5)$ . (1b) Nonlinear stage: The dominant modes are  $(n_x, n_y) = (0, \pm 3)$ . Note the shift to longer wavelength in the nonlinear saturated state.

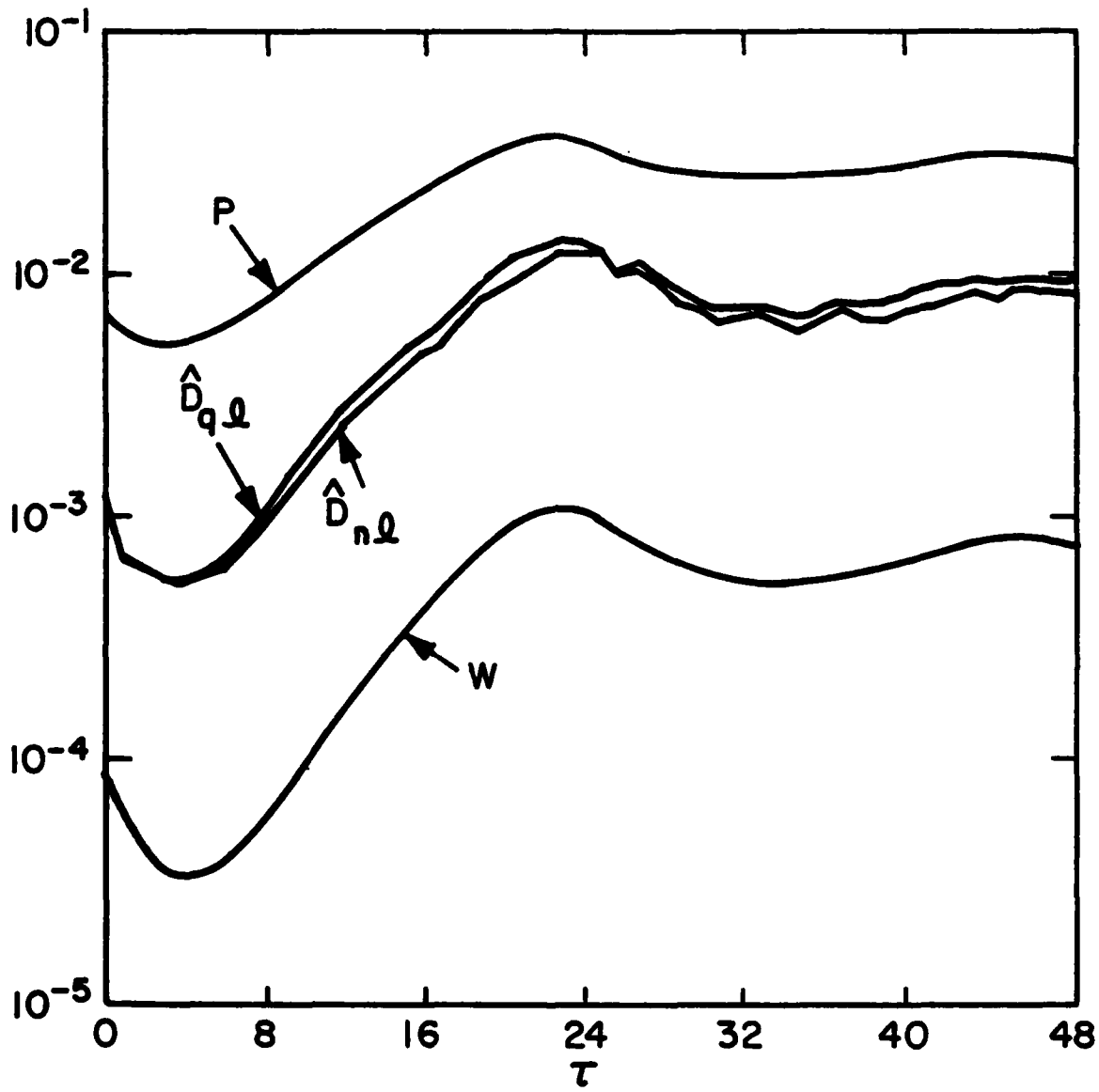


Fig. 2. Time evolution of the wave energy (W), mean square of the potential fluctuations (P), and diffusion coefficients ( $D_{q1}$  - quasilinear;  $D_{n1}$  - nonlinear) for  $\gamma_0 = 0.5$ .

### Acknowledgments

We are very grateful to Dave Fyfe and Glenn Joyce for providing us with their spectral method code. We also thank Dave Montgomery for several helpful discussions. This research has been supported by ONR, and NASA. One of us (JFD) was partially supported by DOE.

### References

1. N.A. Krall and P.C. Liewer, Phys. Rev. A4, 2094 (1971).
2. R.C. Davidson, N.T. Gladd, C.S. Wu, and J.D. Huba, Phys. Fluid 20, 301 (1977).
3. J.F. Drake, J.D. Huba, and N.T. Gladd, submitted to Phys. F is (1982).
4. D. Winske and P.C. Liewer, Phys. Fluids 21, 1017 (1978).
5. J.F. Drake and T.T. Lee, Phys. Fluids 24, 1115 (1981).
6. J.U. Brackbill, D.W. Forslund, K. Quest, and D. Winske (private communication)
7. A. Hasegawa and K. Mima, Phys. Fluids 21, 87 (1978).
8. W. Horton, Phys. Rev. Lett. 37, 1269 (1976).
9. R.E. Waltz, submitted to Phys. Fluids (1982).
10. D. Fyfe and D. Montgomery, Phys. Fluids 22, 246 (1974).
11. D. Fyfe, G. Joyce, and D. Montgomery, J. Plasma Phys. 17, 317 (1977).
12. Orszag, S.A., Stud. Appl. Math. 50, 293 (1971).
13. R.C. Davidson, Phys. Fluids 21, 1017 (1978).
14. J.F. Drake, N.T. Gladd, and J.D. Huba, Phys. Fluids 24, 301 (1981).
15. H.U. Fahrbach, W.Koppendorfer, M. Munich, J. Neuhauser, H. Rohr, G. Schramm, J. Sommer, and E. Holzhauer, Nuc. Fusion 21, 257 (1981).

**FILM**  
**2-83**